Separation of diffracted waves in TI media

Yogesh Arora & Ilya Tsvankin
Center for Wave Phenomena, Colorado School of Mines

Key words: Diffractions, Kirchhoff, Specularity, Anisotropy

ABSTRACT
Imaging diffracted waves can provide useful information about complex subsurface geology and fracture networks. Separation of diffractions from typically more intensive reflected waves can be done based on specularity, which measures deviation from Snell's law. Here, we analyze two formulations of specularity and their applicability to diffraction processing for anisotropic media. We show that the most common definition of specularity, originally introduced for pure modes in isotropic media, remains valid for both pure and converted waves in arbitrarily anisotropic models. The other formulation operates directly with the difference between the slowness projections onto the reflector for the incident and reflected waves. Testing on a VTI (transversely isotropic with vertical symmetry axis) diffraction ramp model demonstrate that both formulations produce satisfactory results for anisotropic media with appropriate tapering of the specularity gathers.

1 INTRODUCTION

Diffractions are caused by heterogeneities with linear dimensions smaller than the seismic wavelength. They can provide valuable information about complex subsurface features such as small-scale faults, fractures, pinch-outs, karst, and rough edges around the salt bodies (Landa, 2010). Diffractions are treated as noise during conventional seismic processing, which is designed for enhancing and imaging of reflected waves.

The main challenge in utilizing diffractions is separating them from reflections, which typically dominate surface seismic data. Khaidukov et al. (2004) separate diffractions in isotropic media by applying focusing and defocusing operators. Fomel et al. (2007) operate on post-stack time sections to separate diffractions using plane-wave destruction filters and perform isotropic velocity analysis based on a measure of focusing. Imaging with diffractions can potentially provide higher-resolution seismic sections (Khaidukov et al., 2004), which can be combined with conventional reflection-based images for improved interpretation (Sturzu et al., 2013; Khaidukov et al., 2004; Moser and Howard, 2008).

Kozlov et al. (2004) apply a weighting function, based on the Fresnel zone around the specular reflected ray, to the Kirchhoff integral to suppress reflections during isotropic migration. However, constructing such weights for anisotropic media is cumbersome. Moser and Howard (2008) propose another approach (called "specularity"), which measures the deviation from Snell's law at the reflection point, to define the weighting function. This approach is used by Sturzu et al. (2013) to create "specularity gathers" for efficient separation of diffraction and reflection energy (Sturzu et al., 2013). Deviation from Snell's law, which governs the specular reflected ray, can be measured in different ways. Although specularity ignores the Fresnel zone contribution to the reflections, specularity gathers overcome this problem and provide efficient method of diffraction separation.

Here, we examine two formulations of specularity, one of which is new, and discuss their applicability for pure and converted waves in general anisotropic media. First, we study the response of these specularity expressions for a simple homogeneous isotropic model. The performance of both formulations in separating and imaging of diffracted waves is illustrated on a VTI diffraction ramp model.

2 THEORY

The Kirchhoff migration integral computes a stack over the diffraction hyperbola. The stack can be restricted to the Fresnel zone (Chen, 2004) by applying a weight function which reduces aliasing in the depth image for coarsely sampled data. If the weight function is designed to suppress the contribution from inside the Fresnel zone, the Kirchhoff integral images nonspecular scattered energy (Kozlov et al., 2004). This weight can be formulated in terms of specularity, which represents a measure of deviation from Snell's law.

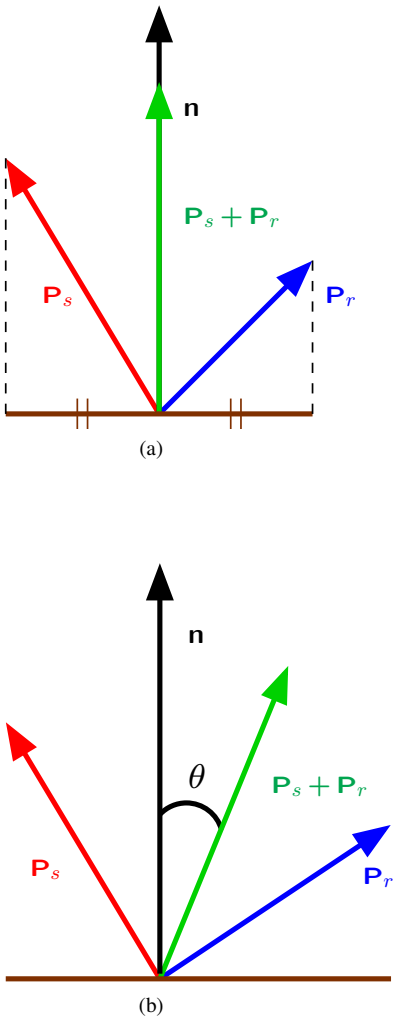

Figure 1. Source slowness vector ($\mathbf{P}_s$), receiver slowness vector ($\mathbf{P}_s$), the sum $\mathbf{P}_s + \mathbf{P}_r$, and the interface normal vector (**n**) for a) the specular reflection, b) a nonspecular diffraction.

Moser and Howard (2008) define specularity as the cosine of the angle between the sum of the source and receiver slowness vectors and the interface normal at the reflection point (Figure 1):

$$S(\mathbf{s},\mathbf{r},\mathbf{X}) = \cos\theta = \frac{(\mathbf{P}_s + \mathbf{P}_r)\cdot\mathbf{n}}{|\mathbf{P}_s + \mathbf{P}_r|}, \tag{1}$$

where S(**s**,**r**,**X**) is the specularity, $\mathbf{P}_s$ and $\mathbf{P}_r$ are the source and receiver slowness vectors obtained from the derivative of source-side traveltime T(**s**,**X**) and receiver-side traveltime T(**r**,**X**), and **n** is the unit vector normal to the reflector. If we assume that the vectors $\mathbf{P}_s$ and $\mathbf{P}_r$ of the specular reflected ray point towards the surface, their projections onto the reflector should cancel according to Snell's law. Therefore, the sum of these slowness vectors is always aligned with the interface normal for specular pure as well as mode-converted waves. Therefore, although the formulation by Moser and Howard (2008) was designed for pure modes in isotropic media, it is entirely valid for arbitrary anisotropy and mode conversions. Alternatively, specularity can be defined directly through the projections of the source and receiver slowness vectors onto the interface (Figure 1). To maintain consistency with equation 1, the sum of these normalized projections can be subtracted from unity:

$$S(\mathbf{s},\mathbf{r},\mathbf{X}) = 1 - \frac{|\mathbf{P}_s\times\mathbf{n} + \mathbf{P}_r\times\mathbf{n}|}{|\mathbf{P}_s + \mathbf{P}_r|}. \tag{2}$$

The value of S in equations 1 and 2 is equal to unity for specular reflections, and is less than unity for non specular events (diffractions). However, reflection energy is formed inside the entire the Fresnel zone where specularity values are generally smaller than unity as well. Therefore, the direct application of a specularity-based weight to the Kirchhoff integral leads to inefficient separation of diffractions.

2.1 Specularity gathers

To overcome this problem, Sturzu et al. (2013) suggest building specularity gathers which, in principle, are similar to surface-offset common-image-gathers (CIGs). The specular and nonspecular events in the data are sorted into gathers according to specularity values, and then a taper function is applied to mute reflections. Finally, stacking over the specularity produces the depth image from diffractions. This process is illustrated by the following equations:

$$V(\mathbf{X},S) = \int \mathrm{U}(t,\mathbf{s},\mathbf{r})\,\delta(t - T(\mathbf{X},\mathbf{s},\mathbf{r}))\,\delta(S-\bar{S})\,\mathrm{d}t\,\mathrm{d}\mathbf{s}\,\mathrm{d}\mathbf{r}\,, \tag{3}$$

$$I(\mathbf{X}) = \int V(\mathbf{X},S)\,\mathrm{d}S\,, \tag{4}$$

$$D(\mathbf{X}) = \int w(\mathbf{X},S)\,V(\mathbf{X},S)\,\mathrm{d}S\,, \tag{5}$$

where V(**X**,S) is a cube (in 2D) with specularity gathers, I(**X**) is the conventional depth image, D(**X**) is the depth image from diffractions, **s** is the source position, **r** is the receiver position, T is the traveltime from the source to the receiver through the reflection point **X**, $\bar{S}$ is specularity defined either in equation 1 or 2, U(**s**,**r**,t) is the recorded data, and w(**X**,S) is the taper function. We apply both definitions of specularity $\bar{S}$ (equations 1 and 2) to separate diffractions using equations 3-5.

3 EXAMPLES

Synthetic data are generated using anisotropic pseudo-acoustic finite-difference code `sfttifd2d`, and unit normal vectors are estimated with code `sfdip` (both from MADAGASCAR). Traveltime tables are created using code `rayt2dan`, and

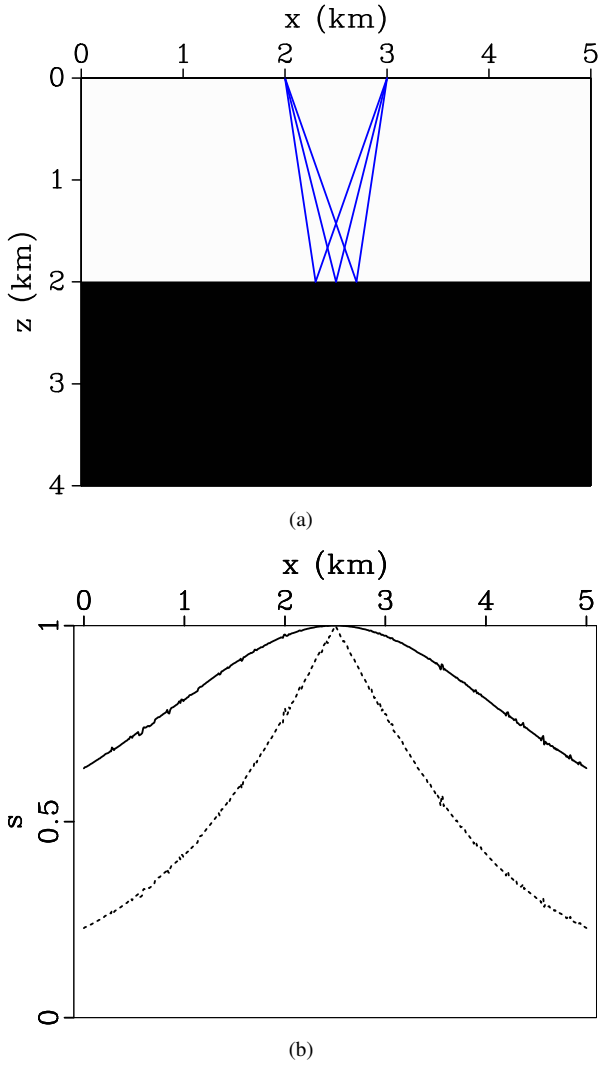

Figure 2. a) Isotropic model with the source and receiver positions fixed at $x = 2$ km and $x = 3$ km, respectively. The reflection point is located at the depth $z = 2$ km and is moved along the horizontal interface. The blue lines represents ray pairs for the moving reflection point. b) The specularity values obtained from equations 1 (solid curve) and 2 (dotted curve).

specularity gathers are built by modified code `sukdmig2d` (both from SEISMIC UNIX).

3.1 Specularity analysis

First, we test the two definitions of specularity for a homogeneous isotropic layer (Figure 2). The specularity is equal to unity for the specular reflection, but it decreases at different rates for the two definitions. The specularity computed from equation 2 decreases faster than that from equation 1, which should cause more smearing in gathers along the specularity axis. Hence, the choice of the taper function $w(\mathbf{X}, \mathrm{S})$ in equation 5 should depend on the definition of specularity.

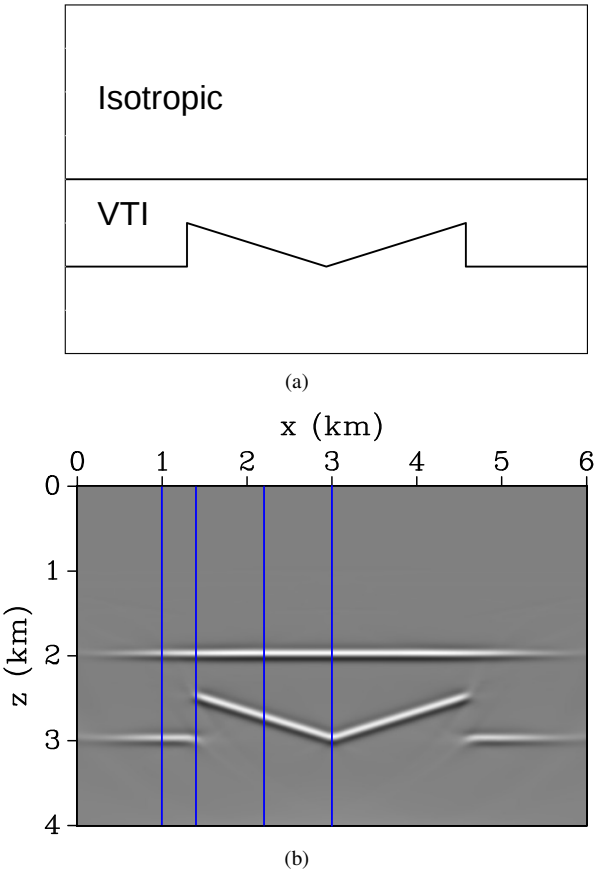

Figure 3. a) VTI diffraction ramp model. b) Conventional depth image of the model. Specularity gathers are computed at locations marked by vertical blue lines.

3.2 VTI diffraction ramp model

Next, we apply the two formulations of specularity to perform separation and imaging of diffraction for a model with a VTI diffraction ramp (Figure 3(a)). The conventional depth image in Figure 3(b) is generated with the actual velocity field, and specularity gathers are constructed at four locations along the line. There are no scatterers at locations $x = 1.0$ km and $x = 2.2$ km, so the corresponding gathers (Figures 4(a) and 4(c)) have no diffracted energy at lower specularity values. However, there is significant nonspecular energy from the scatterers in gathers at locations $x = 1.4$ km and $x = 3.0$ km (Figures 4(b) and 4(d)). As expected, the specularity gathers (Figure 5) computed using equation 2 show more smearing of energy towards lower specularity values. The adjustment of taper function helps produce similar depth images (Figure 7) from diffractions using both definition of specularity.

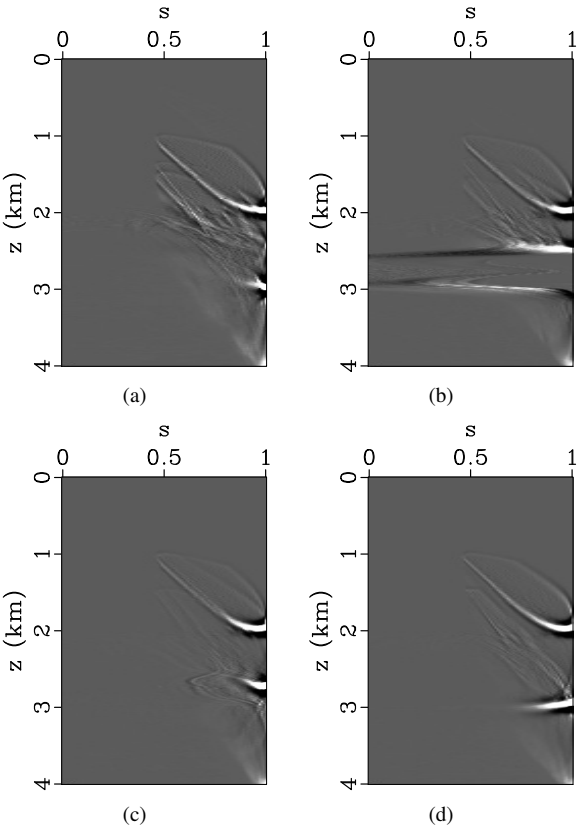

Figure 4. Specularity gathers generated with equation 1 at locations a) $x = 1.0$ km, b) $x = 1.4$ km, c) $x = 2.2$ km, and $x = 3.0$ km.

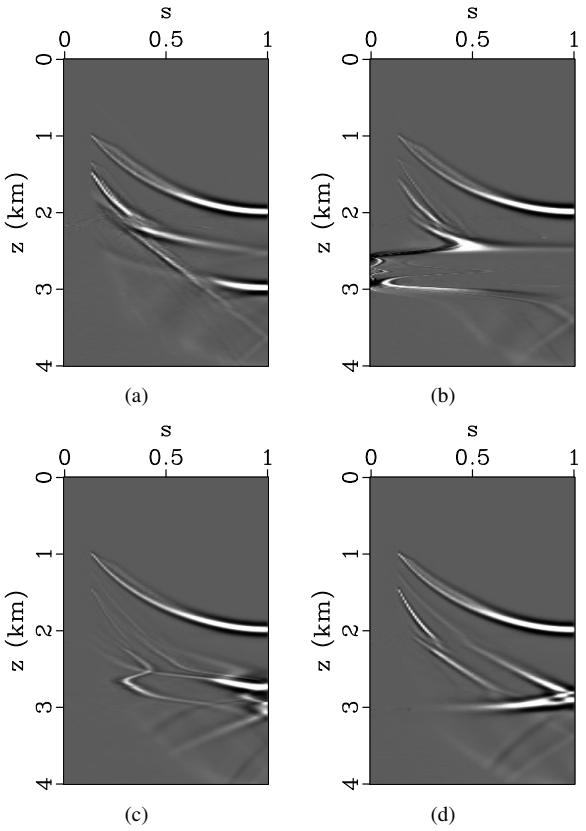

Figure 5. Specularity gathers generated with equation 2 at locations a) $x = 1.0$ km, b) $x = 1.4$ km, c) $x = 2.2$ km, and $x = 3.0$ km.

4 CONCLUSIONS

We applied two formulations of specularity to separate diffractions from reflection data. The difference between these two formulations, illustrated on a simple isotropic model, suggests that tapering should be adjusted depending on the way one computes the specularity. Both formulations are valid for arbitrarily anisotropic media and can be used to generate images with pure-mode and mode-converted diffractions. High-quality diffraction-based depth images for a VTI ramp model illustrate the potential of the presented approach. Ongoing work involves evaluating the stability and accuracy of specularity-based diffraction processing in the presence of errors in the velocity field.

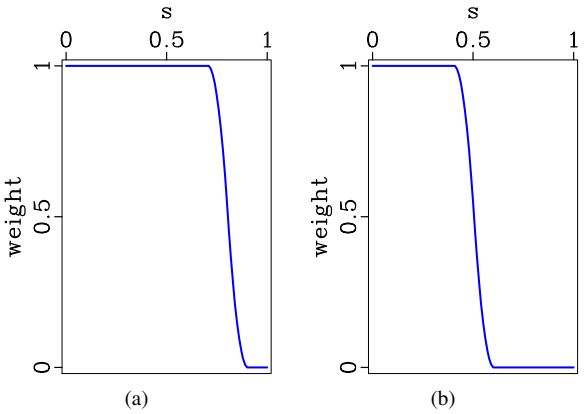

Figure 6. Taper functions with muting starting at a) $S = 0.70$, and b) $S = 0.40$.

5 ACKNOWLEDGMENTS

We are grateful to the members of the A(anisotropy)-Team and iTeam at CWP and to Dr. Tijmen Jan Moser of Moser Geophysical Services for useful discussions. This work was supported by the Consortium Project on Seismic Inverse Methods for Complex Structures at CWP. The reproducible numeric examples in this report are generated with the Madagascar open-source software package freely available from http://www.ahay.org

REFERENCES

Chen, J., 2004, Specular ray parameter extraction and stationary-phase migration: Geophysics, **69**, 249–256.

Fomel, S., E. Landa, and M. Taner, 2007, Poststack velocity analysis by separation and imaging of seismic diffractions: Geophysics, **56**, U89–U94.

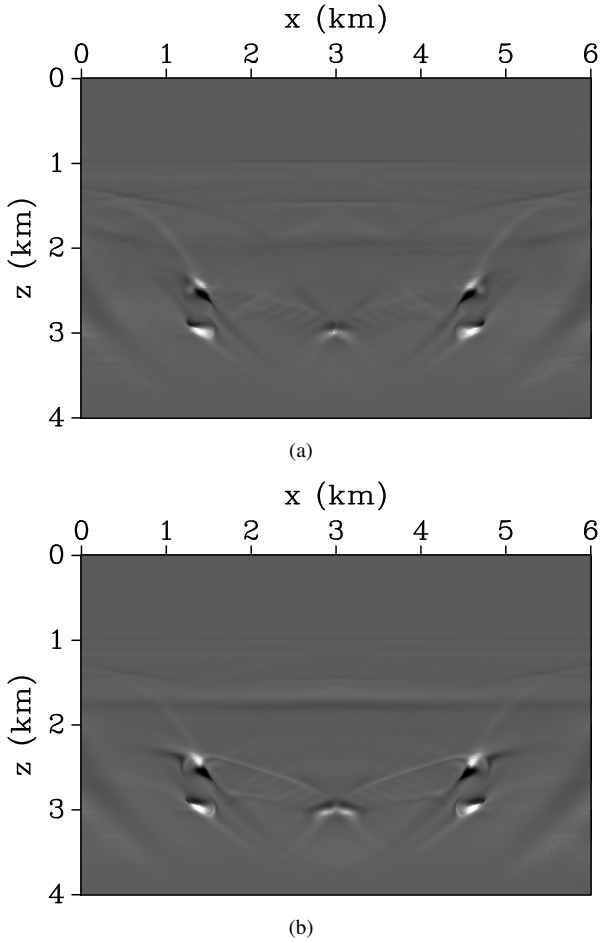

Figure 7. Depth images from diffractions using the specularity defined in a) equation 1 and b) equation 2.

Khaidukov, V., E. Landa, and T. J. Moser, 2004, Diffraction imaging by focusing-defocusing: An outlook on seismic superresolution: Geophysics, **69**, 1478–1490.

Kozlov, E., N. Barasky, E. Korolev, A. Antonenko, and E. Koshchuk, 2004, Imaging scattering objects masked by specular reflections: SEG Technical Program Expanded Abstracts, 1131–1134.

Landa, E., 2010, Diffractions-yesterday, today, and tomorrow: 72nd EAGE Conference & Exhibition, Extended Abstract.

Moser, T. J., and C. B. Howard, 2008, Diffraction imaging in depth: Geophysical Prospecting, **56**, 627–641.

Sturzu, I., A. M. Popovici, N. Tanushev, I. Musat, M. A. Pelissier, and T. J. Moser, 2013, Specularity gathers for diffraction imaging: 75th EAGE Conference & Exhibition, Extended Abstract.